Supplementary Materials for

A sensitive ratiometric fluorescence probe with large spectral shift for sensing and imaging of palladium

Hongyu Li,[abc]* Yue Jian,[abc] Xue Luo,[abc] Yan An,[abc] Mingyan Yang,[abc] Jie Gao,[abc] Junjun Luo,[abc] Xinmin Li, [abc] Jiajia Lv, [abc] Zeli Yuan[abc]*

[a] College of Pharmacy, Zunyi Medical University, Zunyi, Guizhou 563003, China;

[b] Key Laboratory of Basic Pharmacology of Ministry of Education and Joint International Research Laboratory of Ethnomedicine of Ministry of Education, Zunyi Medical University, Zunyi, Guizhou 563000, China;

[c] Guizhou International Scientific and Technological Cooperation Base for Medical Photo-Theranostics Technology and Innovative Drug Development, Zunyi, Guizhou 563003, China.

Table of contents

Synthesis and characterization of the compounds

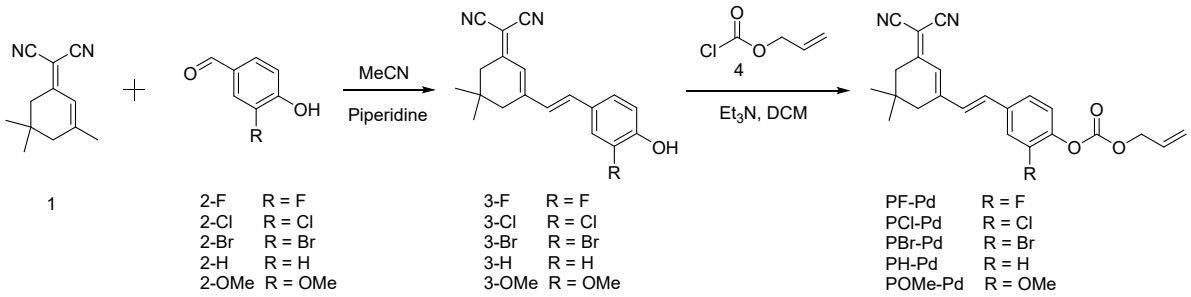

Scheme S1. Synthetic route of the probes.

3-F (orange solid, yield 67 %), ^{1}H NMR (400 MHz, DMSO-d_6): δ 10.43 (s, 1H), 7.61 – 7.54 (m, 1H), 7.33 – 7.22 (m, 2H), 7.17 (d, J = 16.1 Hz, 1H), 6.93 (t, J = 8.7 Hz, 1H), 6.80 (s, 1H), 2.57 (s, 2H), 2.48 (s, 2H), 0.98 (s, 6H). ^{13}C NMR (101 MHz, DMSO-d_6): δ 170.8, 156.7, 152.8, 150.4, 147.1, 137.4, 128.2, 126.1, 122.5, 118.3, 115.1, 114.5, 113.6, 75.9, 42.7, 38.5, 32.1, 27.9. HR-ESI-MS: *m/z* calcd. for C19H16FN2O [M-H]$^{-}$, 307.1252; found, 307.1252.

3-Cl (orange solid, yield 71 %), ^{1}H NMR (400 MHz, DMSO-d_6): δ 10.74 (s, 1H), 7.79 (d, J = 2.0 Hz, 1H), 7.47 (s, 1H), 7.25 (d, J = 32.0 Hz, 2H), 6.98 (d, J = 8.5 Hz, 1H), 6.84 (s, 1H), 2.60 (s, 2H), 2.51 (s, 2H), 1.01 (s, 6H). ^{13}C NMR (101 MHz, DMSO-d_6): δ 170.7, 156.7, 154.9, 137.0, 129.5, 128.9, 128.9, 128.2, 122.5, 120.9, 117.2, 114.5, 113.6, 76.0, 42.7, 38.5, 32.1, 27.9. HR-ESI-MS: *m/z* calcd. for C19H16ClN2O [M-H]$^{-}$, 323.0957; found, 323.0956.

3-Br (orange solid, yield 80 %), ^{1}H NMR (400 MHz, DMSO-d_6): δ 10.82 (s, 1H), 7.93 (d, J = 2.0 Hz, 1H), 7.52 (dd, J = 8.5, 2.0 Hz, 1H), 7.34 – 7.14 (m, 2H), 6.96 (d, J = 8.4 Hz, 1H), 6.84 (s, 1H), 2.59 (s, 2H), 2.50 (s, 2H), 1.00 (s, 6H). ^{13}C NMR (101 MHz, DMSO-d_6): δ 170.72, 156.66, 155.92, 136.91, 132.58, 129.48, 129.35, 128.11, 122.50, 116.92, 114.46, 113.63, 110.57, 75.93, 42.67, 40.53, 40.32, 40.11, 39.90, 39.69, 39.48, 39.27, 38.50, 32.10, 27.88. HR-ESI-MS: *m/z* calcd. for C19H16BrN2O [M-H]$^{-}$, 367.0451; found, 367.0450.

3-H (orange solid, yield 76 %), ^{1}H NMR (400 MHz, DMSO-d_6): δ 10.01 (s, 1H), 7.56 (d, J = 8.4 Hz, 2H), 7.30 – 7.12 (m, 2H), 6.80 (d, J = 6.0 Hz, 3H), 2.59 (s, 2H), 2.52 (s, 2H), 1.01 (s, 6H). ^{13}C NMR (101 MHz, DMSO-d_6): δ 170.7, 159.8, 157.2, 138.7, 130.3, 127.5, 126.7, 121.8, 116.3, 114.6, 113.8, 75.2, 42.7, 38.6, 32.1, 27.9. HR-ESI-MS: *m/z* calcd. for

C19H17N2O [M-H]$^-$, 289.1346; found, 289.1346.

3-OMe (orange solid, yield 69 %), ^{1}H NMR (400 MHz, DMSO-d_6): δ 9.63 (s, 1H), 7.35 (d, J = 1.4 Hz, 1H), 7.31 – 7.17 (m, 2H), 7.10 (dd, J = 8.2, 1.5 Hz, 1H), 6.84 – 6.76 (m, 2H), 3.83 (s, 3H), 2.60 (s, 2H), 2.53 (s, 2H), 1.01 (s, 6H). ^{13}C NMR (101 MHz, DMSO-d_6): δ 170.7, 157.3, 149.3, 148.4, 139.2, 128.1, 126.9, 123.5, 121.7, 116.0, 114.6, 113.9, 110.8, 75.0, 56.0, 42.7, 38.6, 32.1, 27.9. HR-ESI-MS: *m/z* calcd. for C20H19N2O2 [M-H]$^-$, 319.1452; found, 319.1452.

PF-Pd (yellow solid, yield 55 %), ^{1}H NMR (400 MHz, $CDCl_3$): δ 7.36 – 7.31 (m, 1H), 7.29 – 7.25 (m, 2H), 6.95 (d, J = 3.9 Hz, 2H), 6.86 (s, 1H), 6.08 – 5.92 (m, 1H), 5.45 (dd, J = 17.2, 1.3 Hz, 1H), 5.39 – 5.34 (m, 1H), 4.78 (d, J = 5.8 Hz, 2H), 2.61 (s, 2H), 2.46 (s, 2H), 1.09 (s, 6H). ^{13}C NMR (101 MHz, $CDCl_3$): δ 169.01, 155.46, 152.80, 152.32, 139.09, 135.41, 134.38, 130.63, 124.42, 123.83, 123.72, 119.89, 115.28, 115.09, 113.25, 112.47, 79.69, 69.86, 42.95, 39.17, 32.04, 28.01. HR-ESI-MS: *m/z* calcd. for C23H22FN2O3 [M+H]$^+$, 393.1609; found, 393.1610.

PCl-Pd (yellow solid, yield 60 %), ^{1}H NMR (400 MHz, $CDCl_3$): δ 7.59 (d, J = 2.0 Hz, 1H), 7.42 (dd, J = 8.5, 2.0 Hz, 1H), 7.27 (d, J = 7.3 Hz, 1H), 6.95 (s, 2H), 6.87 (s, 1H), 6.06 – 5.96 (m, 1H), 5.46 (dd, J = 17.2, 1.3 Hz, 1H), 5.36 (dd, J = 10.4, 1.1 Hz, 1H), 4.78 (dt, J = 5.8, 1.2 Hz, 2H), 2.61 (s, 2H), 2.45 (s, 2H), 1.09 (s, 6H). ^{13}C NMR (101 MHz, $CDCl_3$): δ 169.0, 152.8, 152.3, 147.6, 135.2, 134.1, 130.7, 129.1, 127.6, 126.7, 124.4, 123.7, 119.8, 113.2, 112.4, 79.7, 69.8, 42.9, 39.1, 32.0, 28.0. HR-ESI-MS: *m/z* calcd. for C23H22ClN2O3 [M+H]$^+$, 409.1313; found, 409.1317.

PBr-Pd (yellow solid, yield 59 %), ^{1}H NMR (400 MHz, $CDCl_3$): δ 7.76 (d, J = 1.9 Hz, 1H), 7.47 (dd, J = 8.5, 2.0 Hz, 1H), 7.27 (d, J = 2.8 Hz, 1H), 6.95 (s, 2H), 6.86 (s, 1H), 6.06 – 5.96 (m, 1H), 5.50 – 5.41 (m, 1H), 5.38 – 5.31 (m, 1H), 4.79 (d, J = 5.8 Hz, 2H), 2.61 (s, 2H), 2.45 (s, 2H), 1.09 (s, 6H). ^{13}C NMR (101 MHz, $CDCl_3$): δ 169.0, 152.8, 152.3, 148.8, 135.5, 133.9, 132.2, 130.7, 127.4, 124.5, 123.7, 119.9, 116.7, 113.2, 112.5, 79.7, 69.8, 42.9, 39.1, 32.0, 28.0. HR-ESI-MS: *m/z* calcd. for C23H22BrN2O3 [M+H]$^+$, 453.0808; found, 453.0813.

PH-Pd (yellow solid, yield 67 %), ^{1}H NMR (400 MHz, $CDCl_3$): δ 7.53 (d, J = 8.7 Hz, 2H), 7.23 (d, J = 8.7 Hz, 2H), 7.07 – 6.91 (m, 2H), 6.85 (s, 1H), 6.04 – 5.97 (m, 1H), 5.49 –

5.31 (m, 2H), 4.76 (dt, J = 5.9, 1.2 Hz, 2H), 2.61 (s, 2H), 2.47 (s, 2H), 1.09 (s, 6H). ^{13}C NMR (101 MHz, $CDCl_3$): δ 169.2, 153.5, 153.1, 151.8, 135.6, 133.6, 130.9, 129.5, 128.6, 123.8, 121.7, 119.8, 113.4, 112.6, 79.0, 69.4, 43.0, 39.2, 32.0, 28.0. HR-ESI-MS: *m/z* calcd. for C23H23N2O3 $[M+H]^+$, 375.1703; found, 375.1714.

POMe-Pd (yellow solid, yield 48 %), ^{1}H NMR (400 MHz, $CDCl_3$): δ 7.17 – 7.11 (m, 2H), 7.07 (dd, J = 8.2, 1.8 Hz, 1H), 7.02 (d, J = 16.1 Hz, 1H), 6.94 (d, J = 16.1 Hz, 1H), 6.86 (s, 1H), 6.05 – 5.95 (m, 1H), 5.44 (dq, J = 17.2, 1.4 Hz, 1H), 5.33 (dd, J = 10.4, 1.2 Hz, 1H), 4.75 (d, J = 5.8 Hz, 2H), 3.92 (s, 3H), 2.61 (s, 2H), 2.47 (s, 2H), 1.09 (s, 6H). ^{13}C NMR (101 MHz, $CDCl_3$): δ 169.3, 153.6, 152.8, 151.5, 141.1, 136.0, 134.9, 131.0, 129.5, 123.8, 122.8, 120.8, 119.3, 113.4, 112.7, 110.4, 78.8, 69.4, 56.0, 42.9, 39.1, 32.0, 28.0. HR-ESI-MS: *m/z* calcd. for C24H25N2O4 $[M+H]^+$, 405.1809; found, 405.1817.

Comparison of PF-Pd with some recently reported ratiometric probes for Pd

Table S1. Comparison of PF-Pd with some recently reported ratiometric probes for Pd

Structure	Analyte	Detection wavelength (Spectral shift)	LOD	Application	Ref.
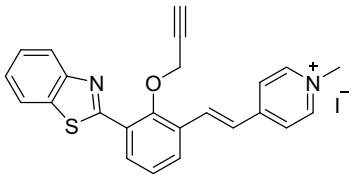	Pd^0 Pd^{2+} Pd^{4+}	495 nm to 635 nm (140 nm)	57 nM	Not mentioned	1
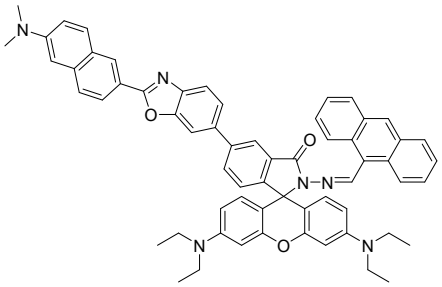	Pd^{2+}	495 nm to 595 nm (100 nm)	230 nM	Cell imaging Tissue imaging	2
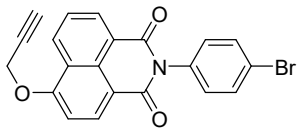	Pd^{2+}	445 nm to 550 nm (105 nm)	280 nM	Cell imaging Tissue imaging	3
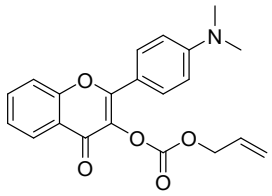	Pd^0 Pd^{2+} Pd^{4+}	470 nm to 552 nm (82 nm)	9.0 nM	Cell imaging Tissue imaging	4
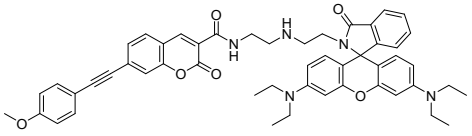	Pd^{2+}	515 nm to 575 nm (60 nm)	Not mention-ed	Cell imaging Tissue imaging Zebrafish imaging	5
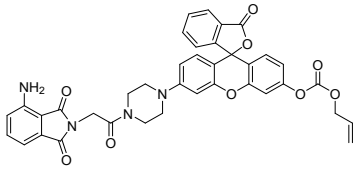	Pd^0	490 nm to 547 nm (57 nm)	31 nM	Cell imaging	6

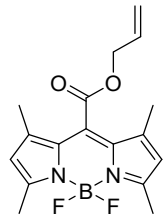	Pd^0	591 nm to 513 nm (78 nm)	7.4 nM	Cell imaging	7
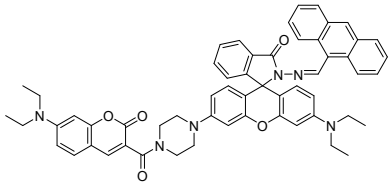	Pd^{2+}	472 nm to 594 nm (122 nm)	Not mention -ed	Cell imaging	8
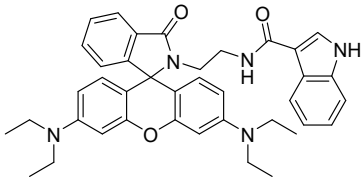	Pd^{2+}	410 nm to 590 nm (180 nm)	170 nM	Cell imaging	9
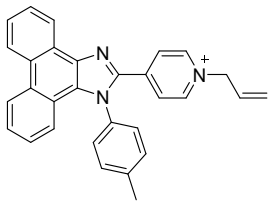	Pd^0	520 nm to 410 nm (110 nm)	8.46 nM	Practical water assay	10
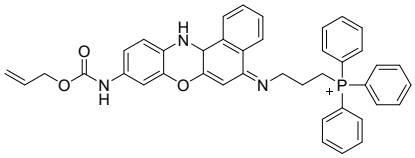	Pd^0	590 nm to 640 nm (50 nm)	5.8 nM	Cell imaging	11
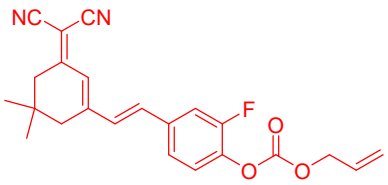	Pd^0	517 nm to 665 nm (148 nm)	2.11 nM	Colorimetric assay Test strip Practical water assay Practical soil assay Cell imaging	This work

Spectroscopic measurement of Pd^0

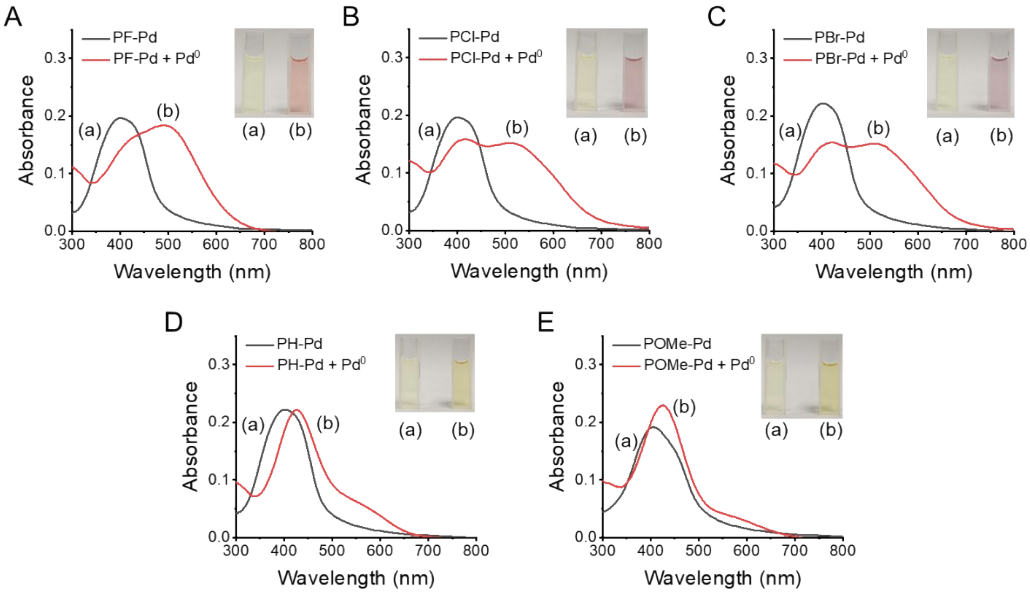

Fig. S1. Absorption spectra of 10 μM probe (a) before and (b) after treated with 5 μM $Pd(PPh_3)_4$ in pH 7.4 phosphate buffer (10 mM, 20% DMSO).

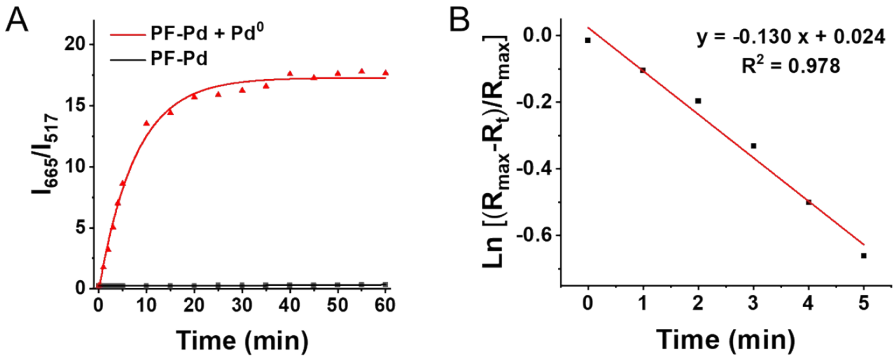

Fig. S2. (A) Effects of reaction time on the fluorescence ratio (I_{665}/I_{517}) of 10 μM PF-Pd in the absence (black) and presence (red) of 3 μM $Pd(PPh_3)_4$ in pH 7.4 phosphate buffer (10 mM, 20% DMSO). (B) The $Ln[(R_{max}-R_t)/R_{max}]$~t plot within 5 min, where R_{max} is the maximum of I_{665}/I_{517}, R_t is I_{665}/I_{517} of indicated time.

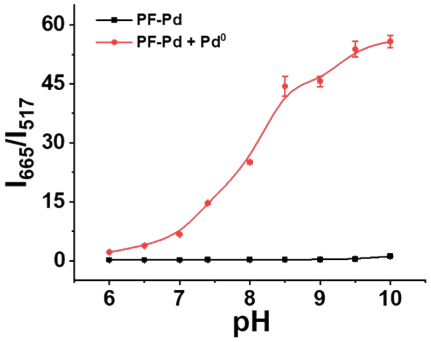

Fig. S3. Ratio (I_{665}/I_{517}) of PF-Pd (10 μM) in phosphate buffer (10 mM, 20% DMSO) with different pH in the absence cc(black) and presence (red) of 3 μM $Pd(PPh_3)_4$. λ_{ex} = 440 nm.

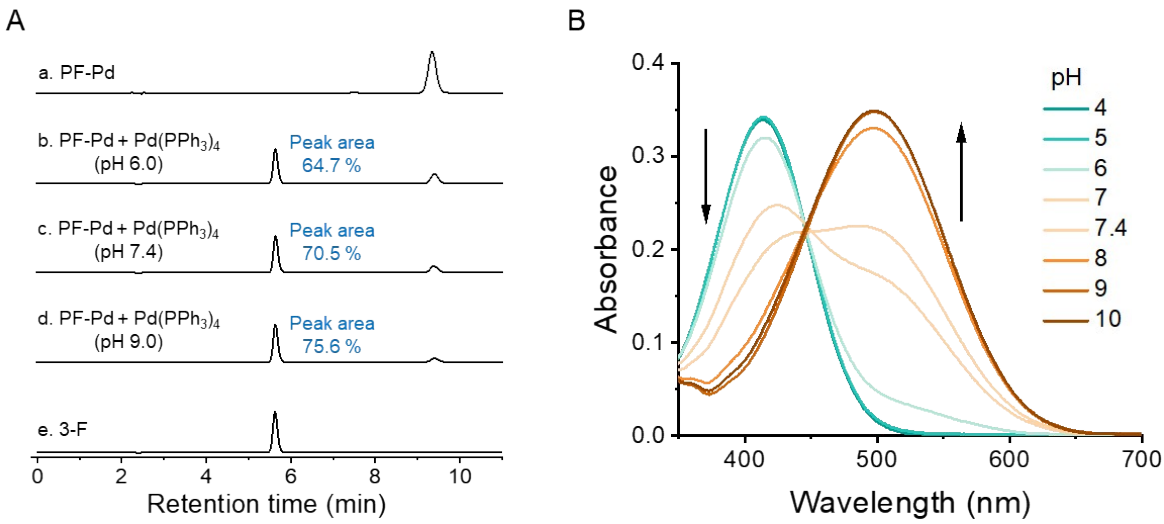

Fig. S4. (A) Chromatograms of different systems: (a) PF-Pd; (b-d) PF-Pd reacting with $Pd(PPh_3)_4$ in (b) pH 6.0, (c) pH 7.4 or (d) pH 9.0 phosphate buffer; (e) Prepared 3-F. The chromatography peaks were recorded by the absorbance at 440 nm (isoabsorptive point) with mobile phase of 80% MeOH and 20 % H_2O (0.1 % TFA). (B) Absorption spectra of 3-F under different pH.

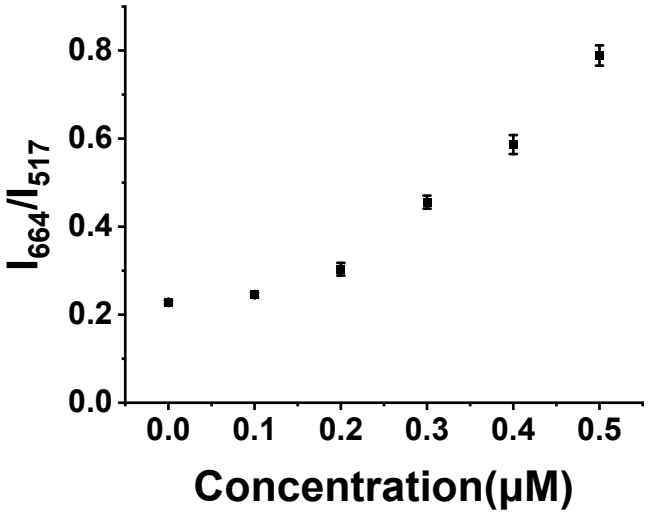

Fig. S5. Ratio (I_{665}/I_{517}) of PF-Pd (10 μM) in phosphate buffer (10 mM, 20% DMSO) with low concentrations of $Pd(PPh_3)_4$. λ_{ex} = 440 nm.

Colorimetric analysis of Pd^0 by PF-Pd

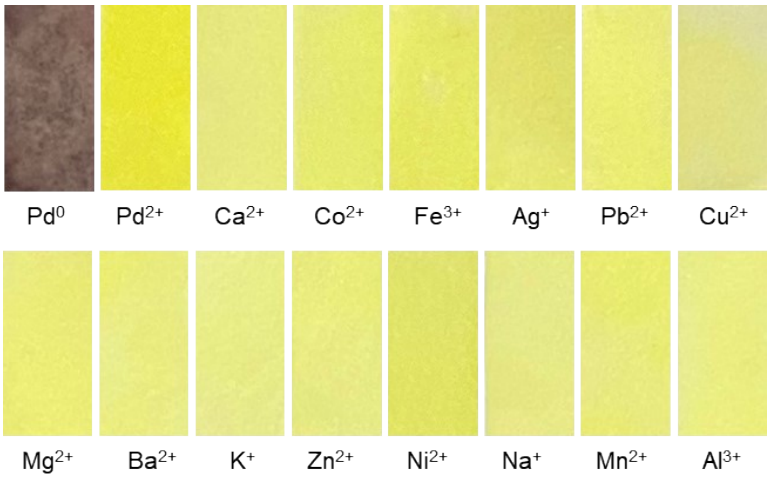

Fig. S6. Color changes of the PF-Pd loaded test strips in response to1 mM of different metal ions.

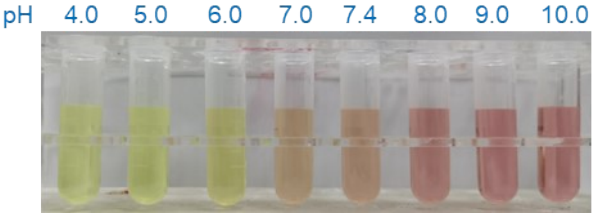

Fig. S7. Color of 3-F at different pH conditions.

Biocompatibility of PF-Pd

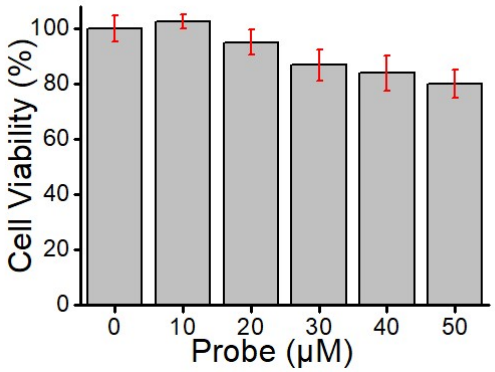

Fig. S8. The viability of 4T1 cells after treated with various amount of PF-Pd for 24 h. The viability of cells without PF-Pd is defined as 100%. The results are presented as mean ± standard deviation (n = 6).

Fluorescence imaging

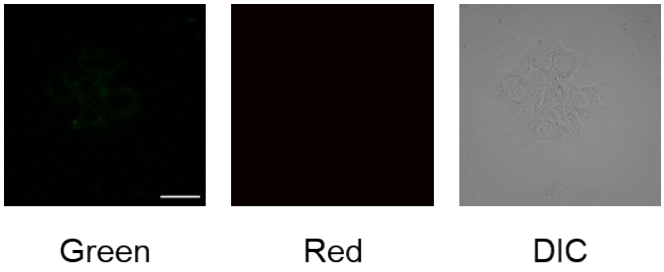

Fig. S9. Fluorescence and DIC images of blank 4T1 cells. Green channel: λ_{ex} = 405 nm, λ_{em} = 480 nm-550 nm; red channel: λ_{ex} = 405 nm, λ_{em} = 620 nm-680 nm. Scale bar: 200 μM.

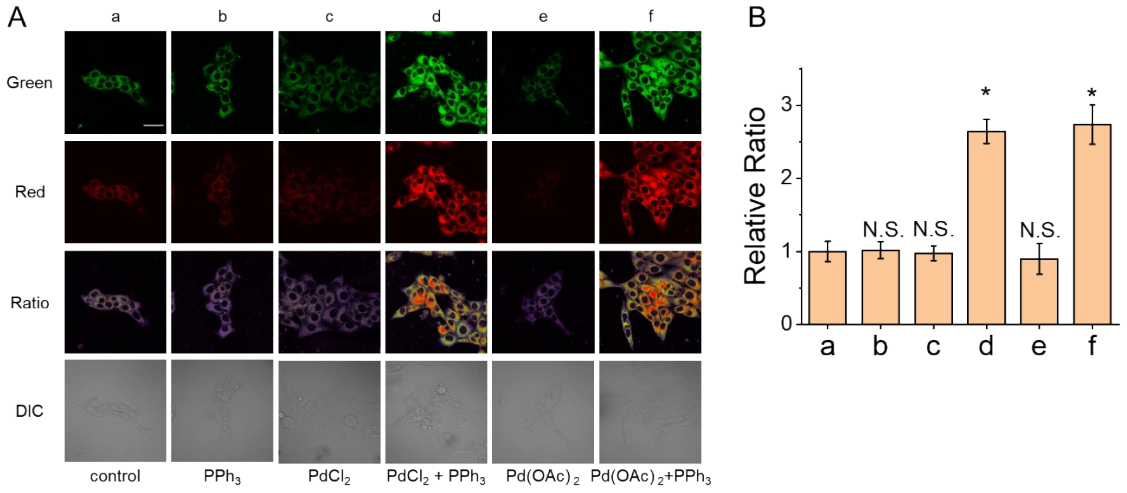

Fig. S10. (A) Fluorescence and DIC images of 4T1 cells under different conditions. (a) Cells treated with 10 μM PF-Pd for 30 min. (b-f) Cells pretreated with 10 μM PF-Pd for 30 min, then incubated with (b) 20 μM PPh_3, (c) 5 μM $PdCl_2$, (d) 5 μM $PdCl_2$ + 20 μM PPh_3, (e) 5 μM $Pd(OAc)_2$ or (f) 5 μM $Pd(OAc)_2$ + 20 μM PPh_3 for 30 min. Green channel: λ_{ex} = 405 nm, λ_{em} = 480 nm-550 nm; red channel: λ_{ex} = 405 nm, λ_{em} = 620 nm-680 nm. Scale bar: 200 μM. (B) Relative ratio of the fluorescence images from panel A (ratio of image a is defined as 1.0). The results are presented as mean ± standard deviation (n = 3). Significant differences compared to image a (N.S.: no significant difference; *$p < 0.05$) are performed by Student's *t*-test.

NMR spectra of the compounds

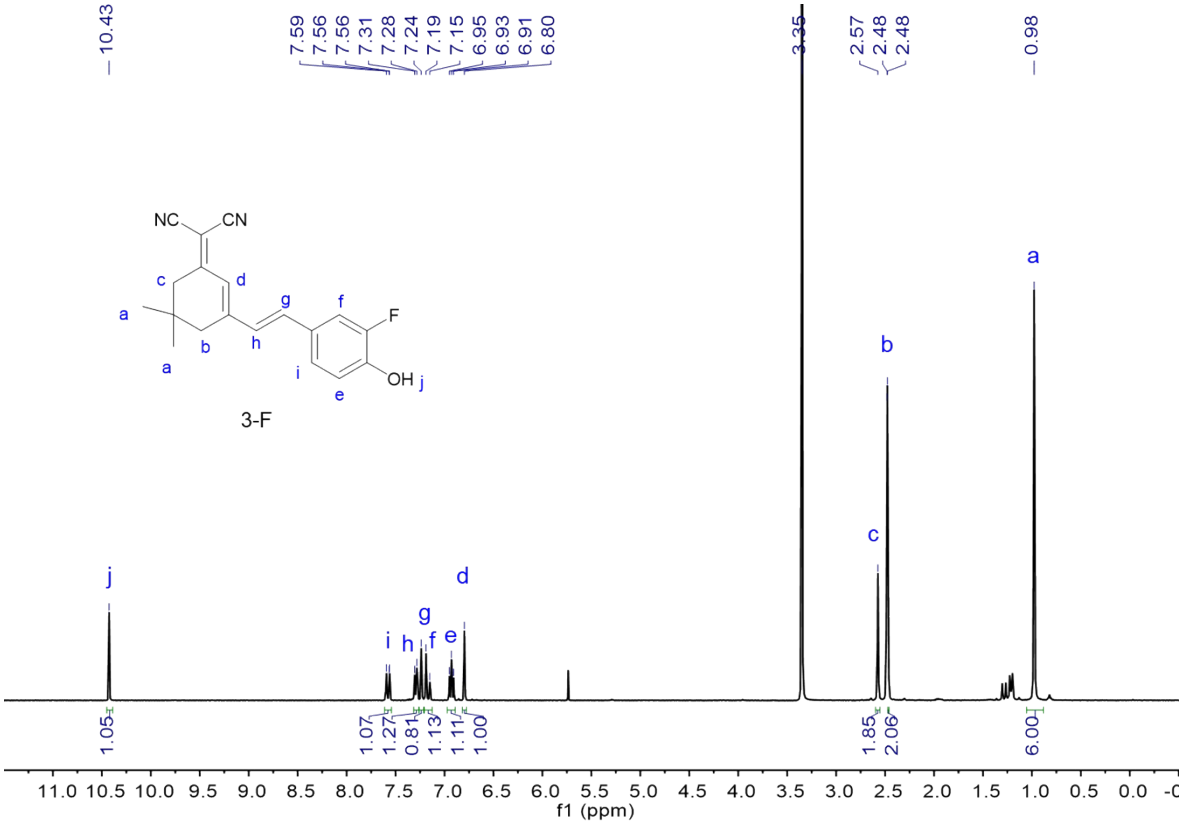

Fig. S11. ^{1}H NMR spectrum of 3-F in DMSO-d_6 (400 MHz, 298 K).

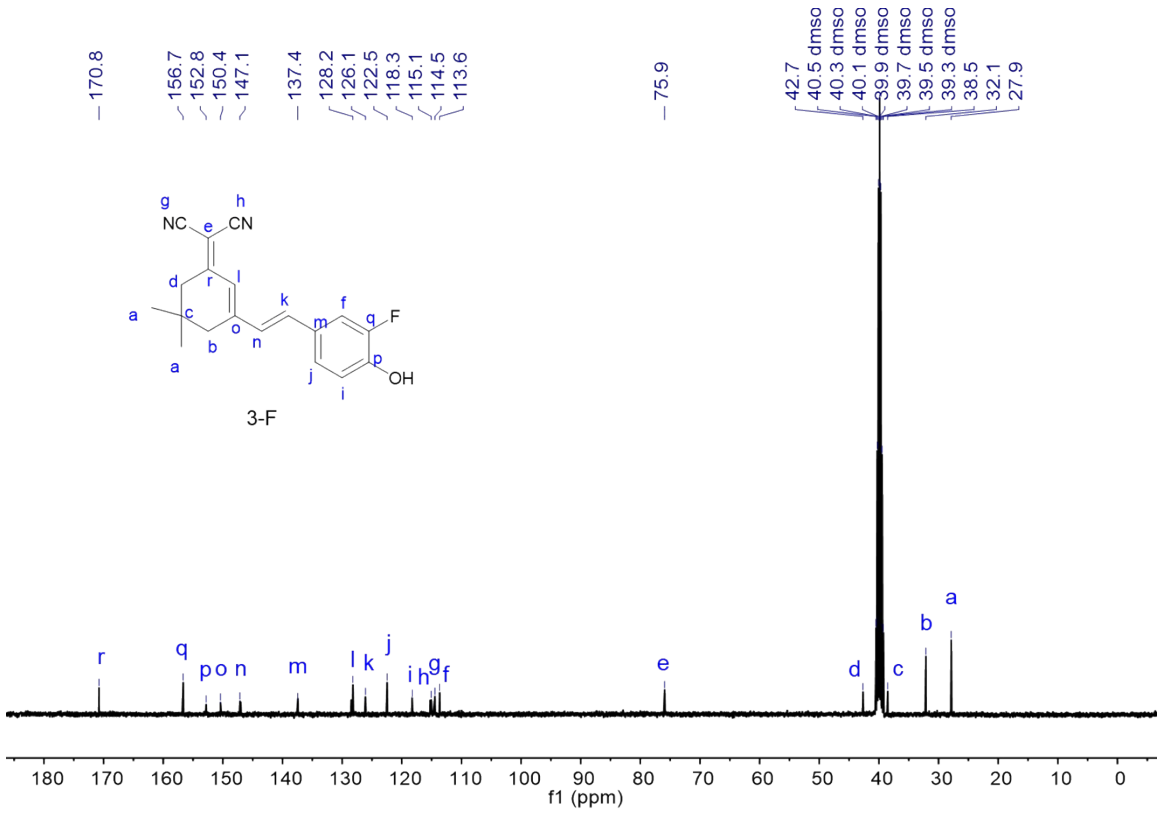

Fig. S12. ^{13}C NMR spectrum of 3-F in DMSO-d_6 (100 MHz, 298 K).

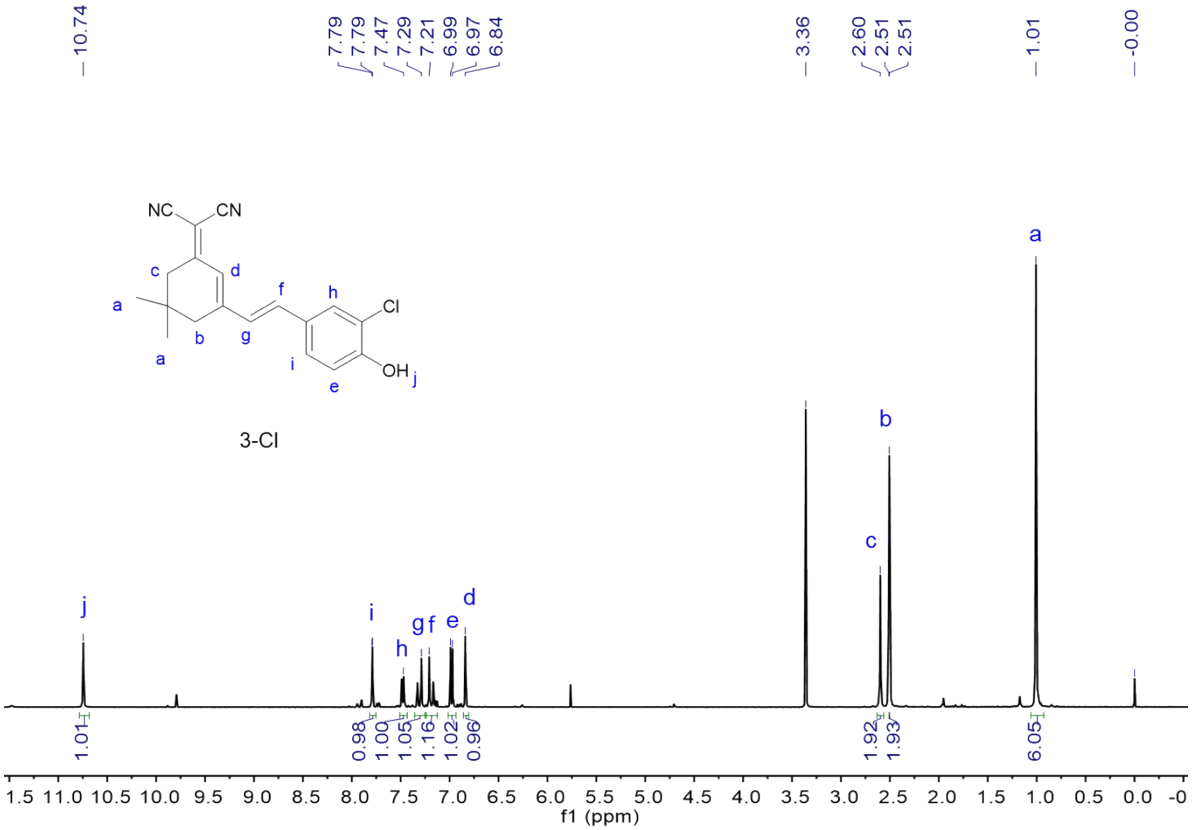

Fig. S13. [1]H NMR spectrum of 3-Cl in DMSO-d_6 (400 MHz, 298 K).

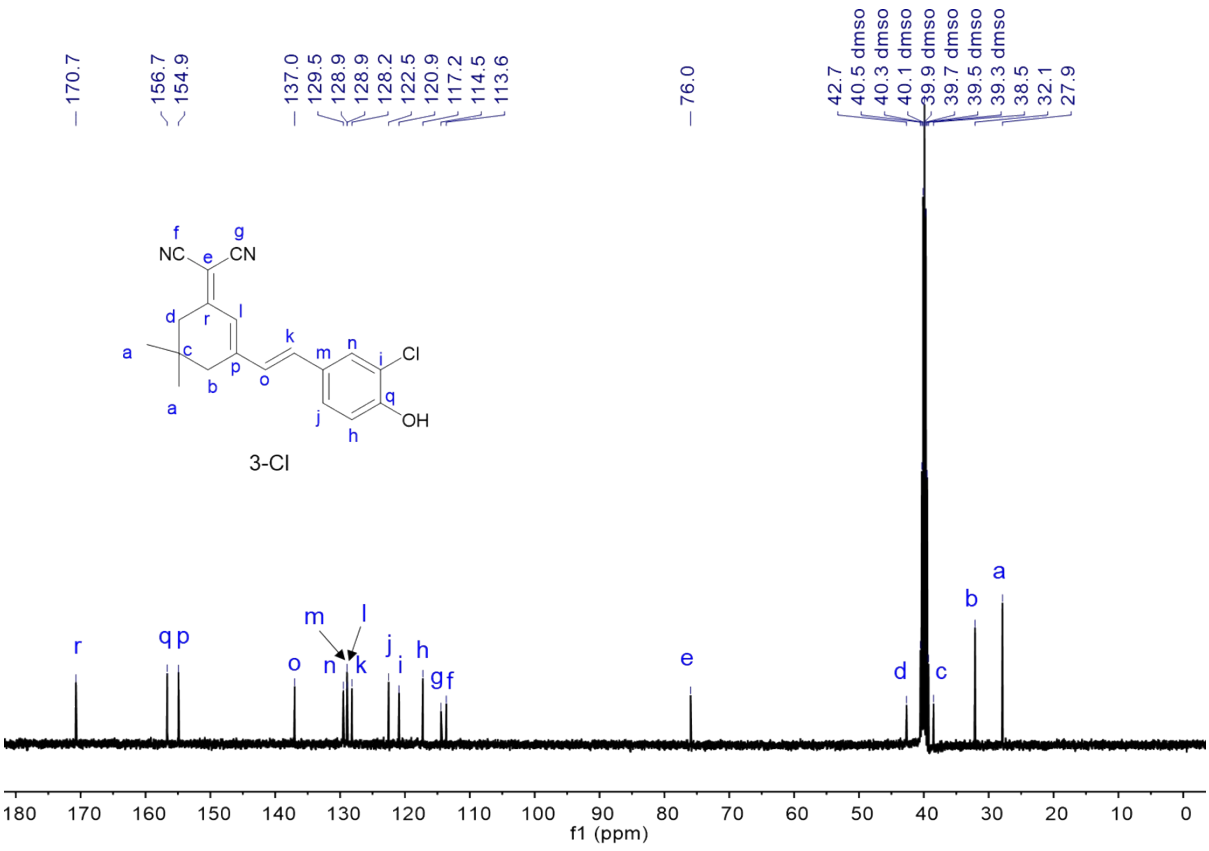

Fig. S14. [13]C NMR spectrum of 3-Cl in DMSO-d_6 (100 MHz, 298 K).

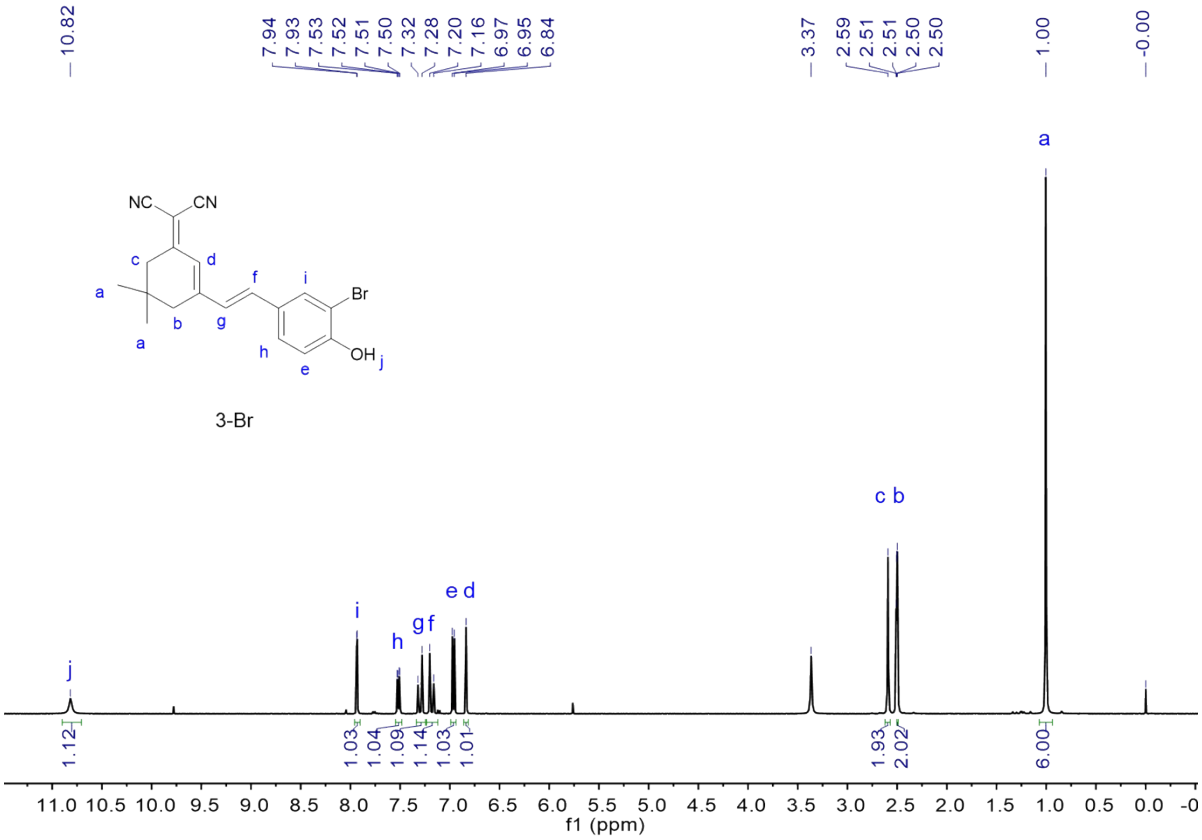

Fig. S15. ^{1}H NMR spectrum of 3-Br in DMSO-d_6 (400 MHz, 298 K).

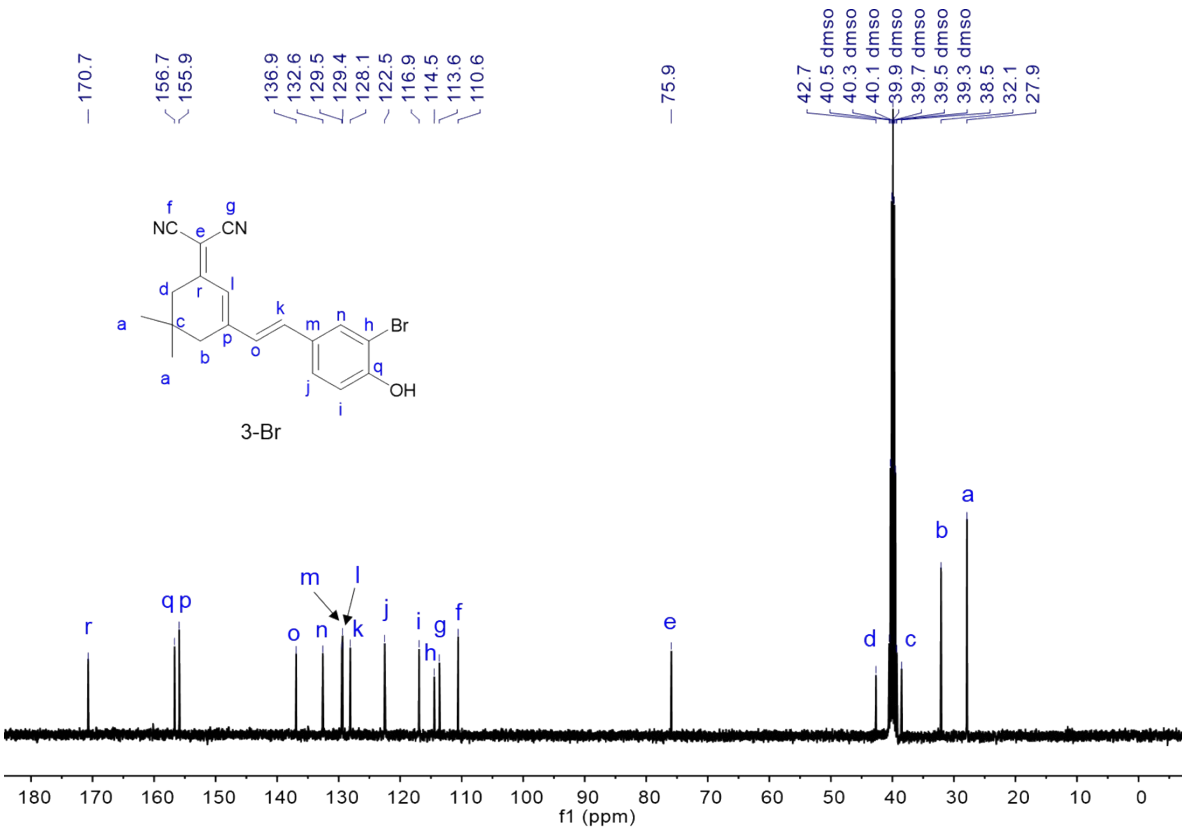

Fig. S16. ^{13}C NMR spectrum of 3-Br in DMSO-d_6 (100 MHz, 298 K).

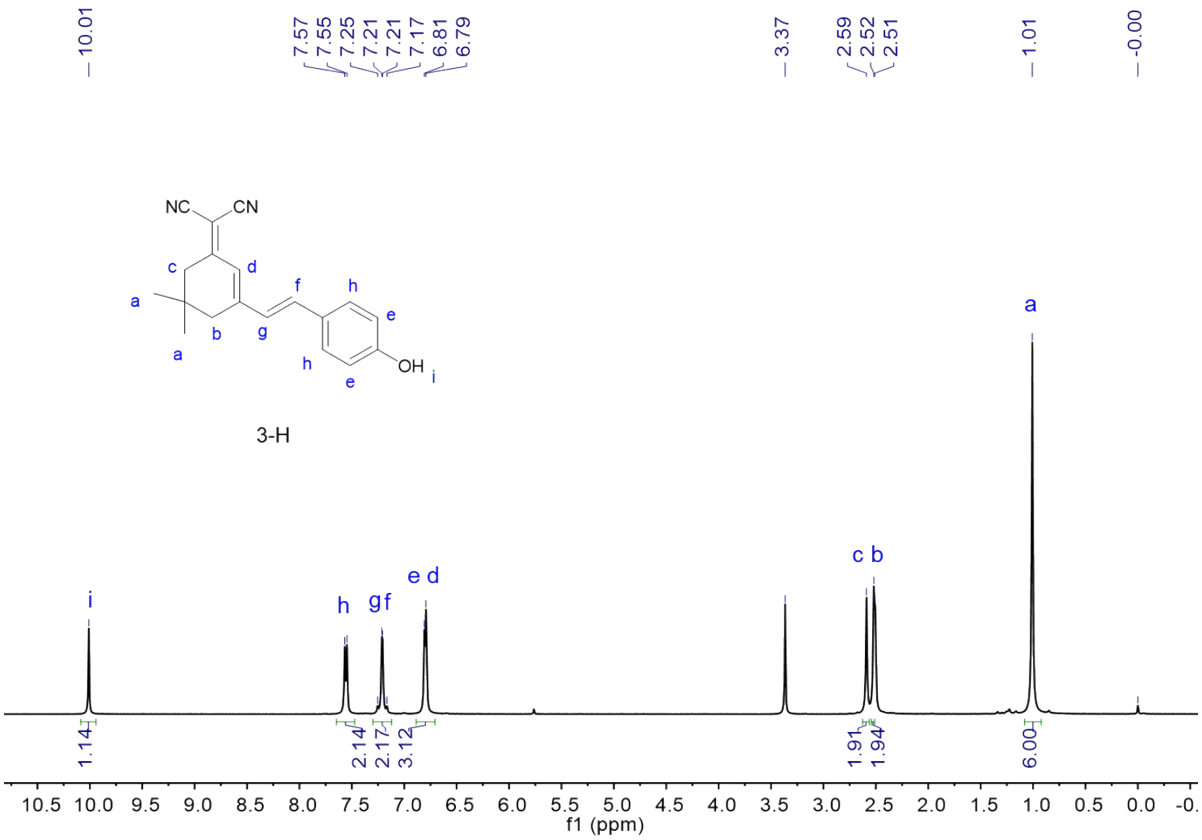

Fig. S17. ^{1}H NMR spectrum of 3-H in DMSO-d_6 (400 MHz, 298 K).

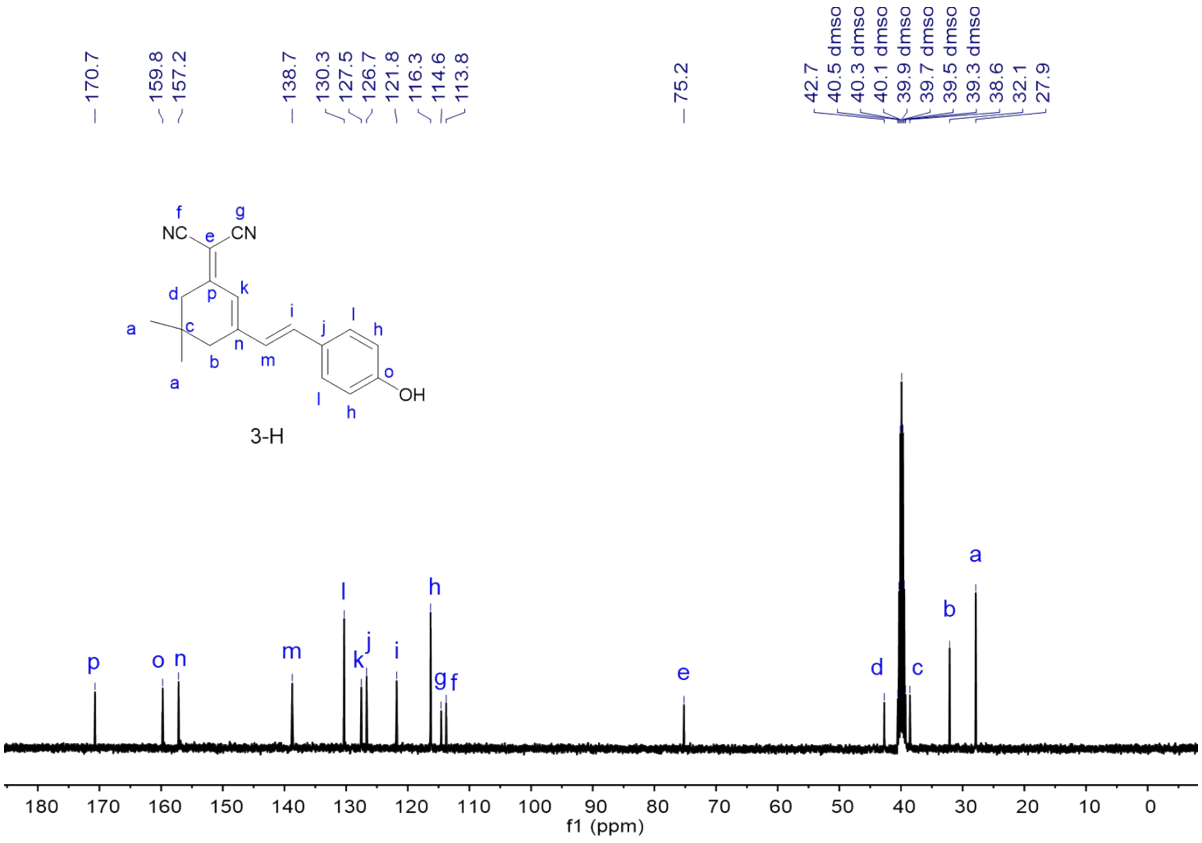

Fig. S18. ^{13}C NMR spectrum of 3-H in DMSO-d_6 (100 MHz, 298 K).

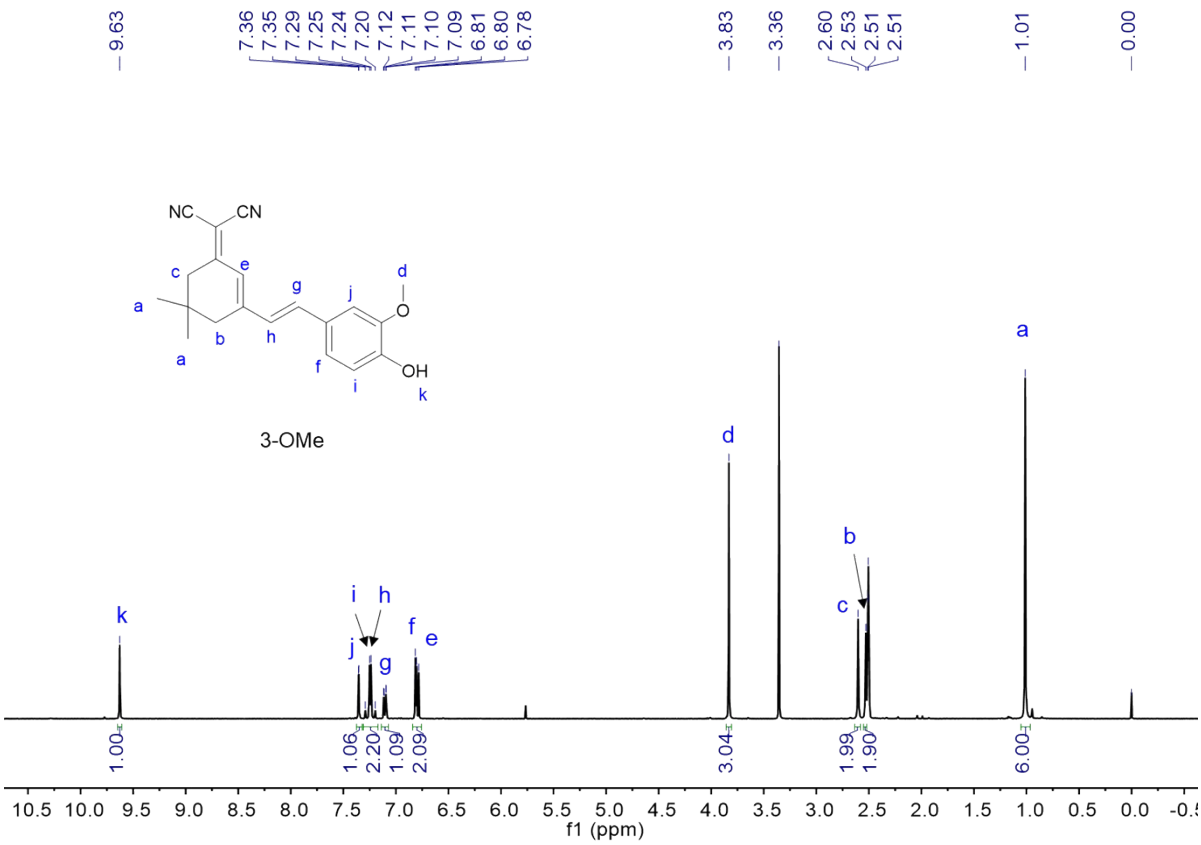

Fig. S19. [1]H NMR spectrum of 3-OMe in DMSO-d_6 (400 MHz, 298 K).

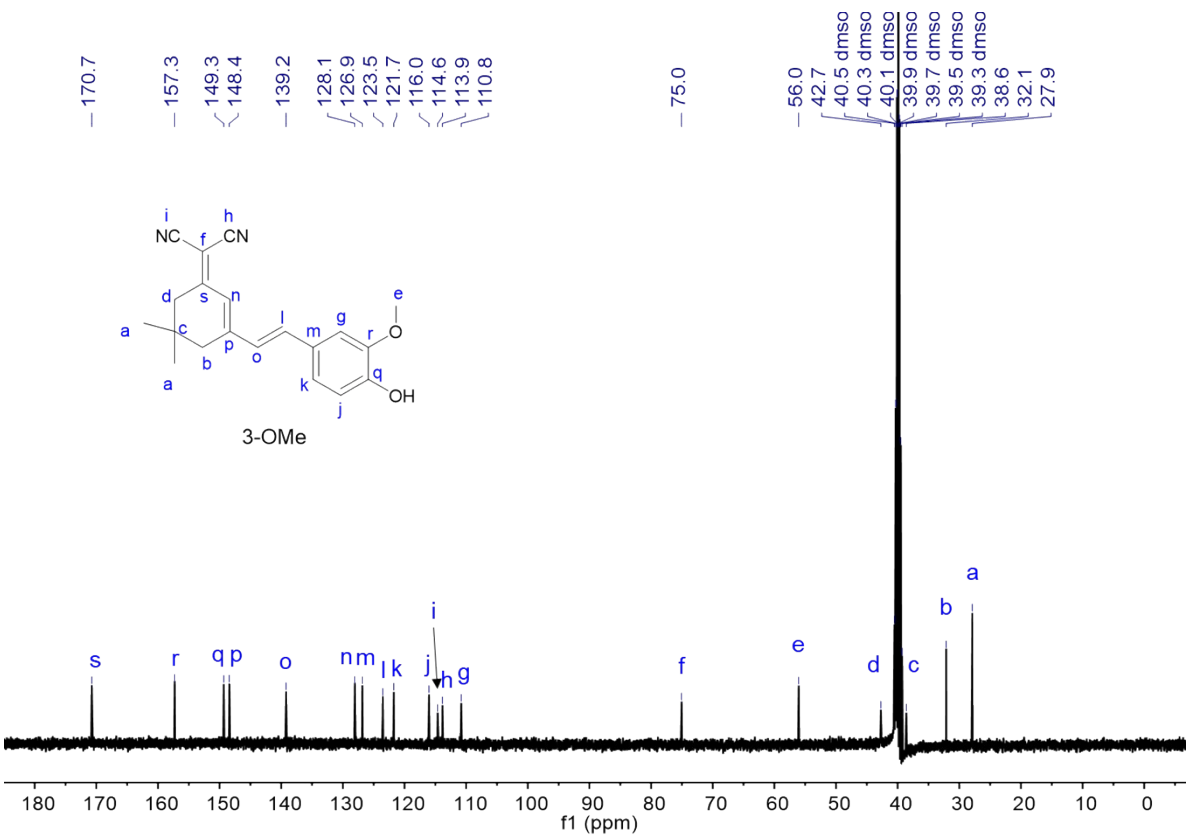

Fig. S20. [13]C NMR spectrum of 3-OMe in DMSO-d_6 (100 MHz, 298 K).

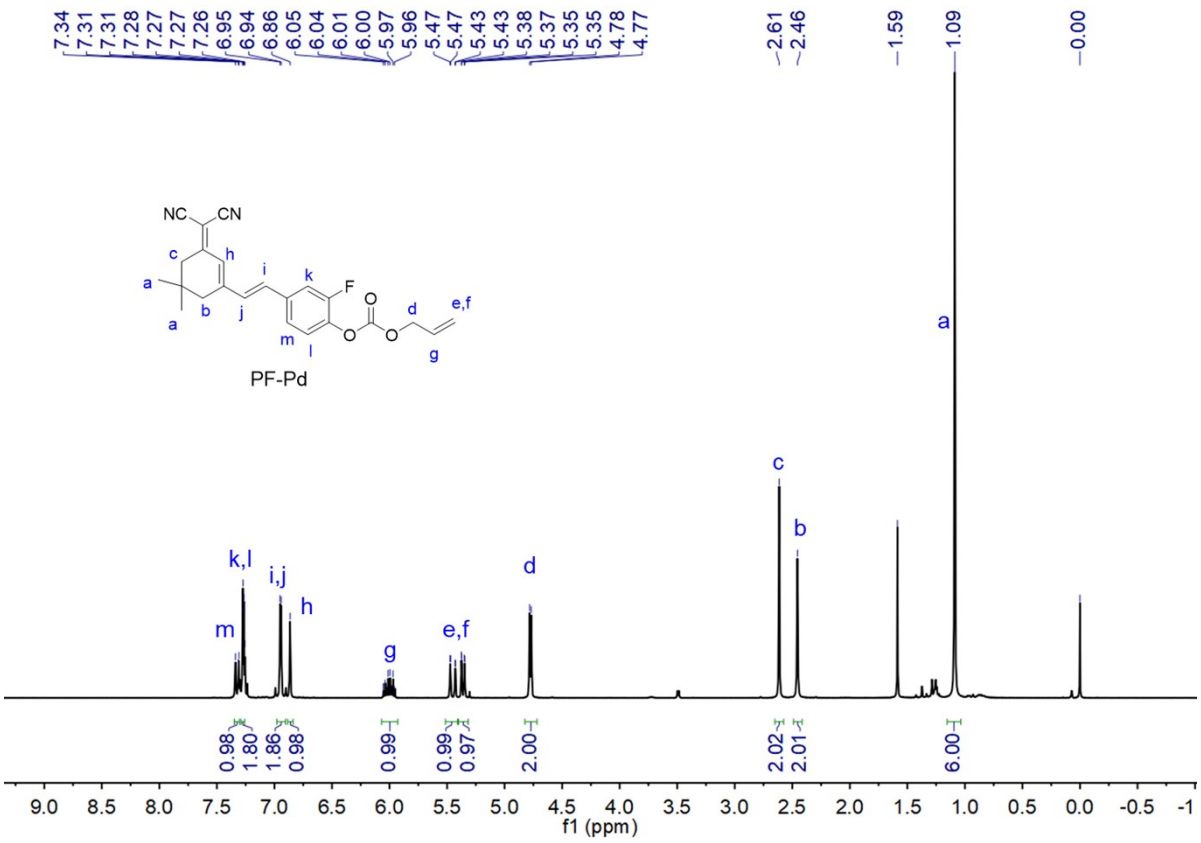

Fig. S21. ^{1}H NMR spectrum of PF-Pd in $CDCl_3$ (400 MHz, 298 K).

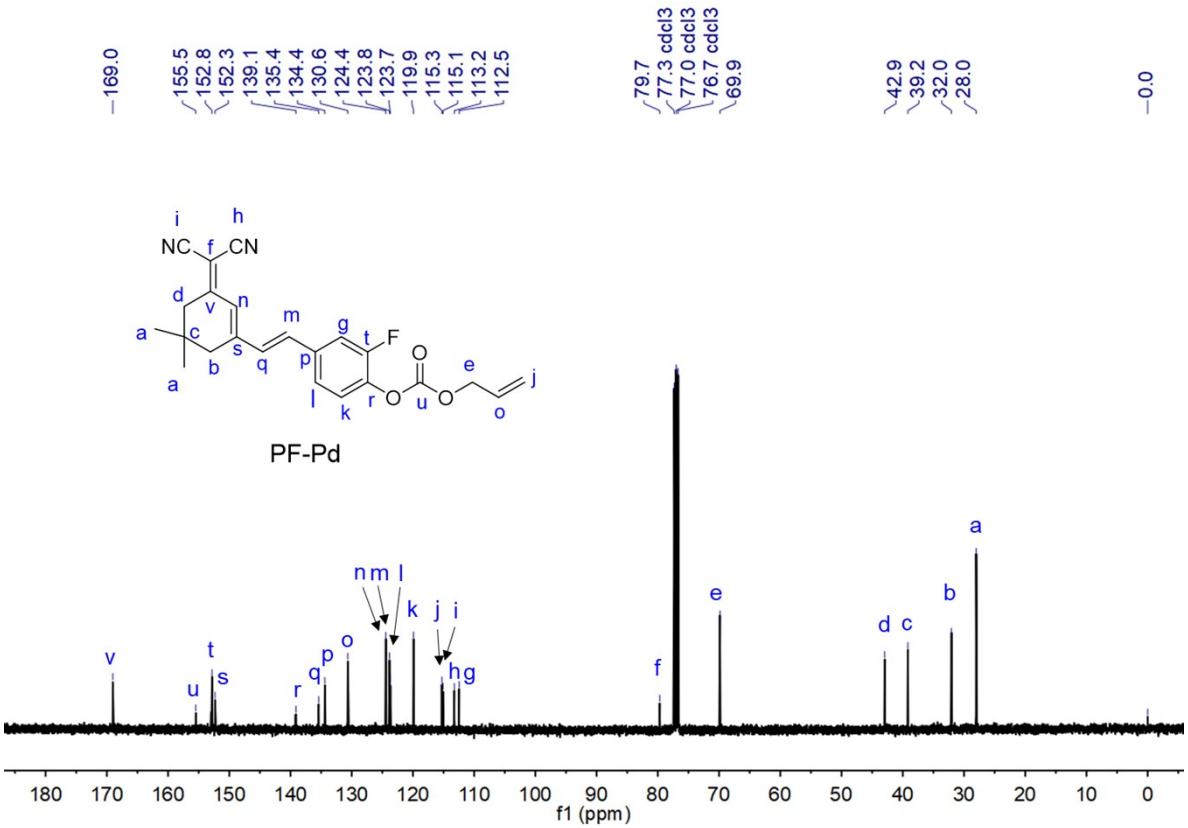

Fig. S22. ^{13}C NMR spectrum of PF-Pd in $CDCl_3$ (100 MHz, 298 K).

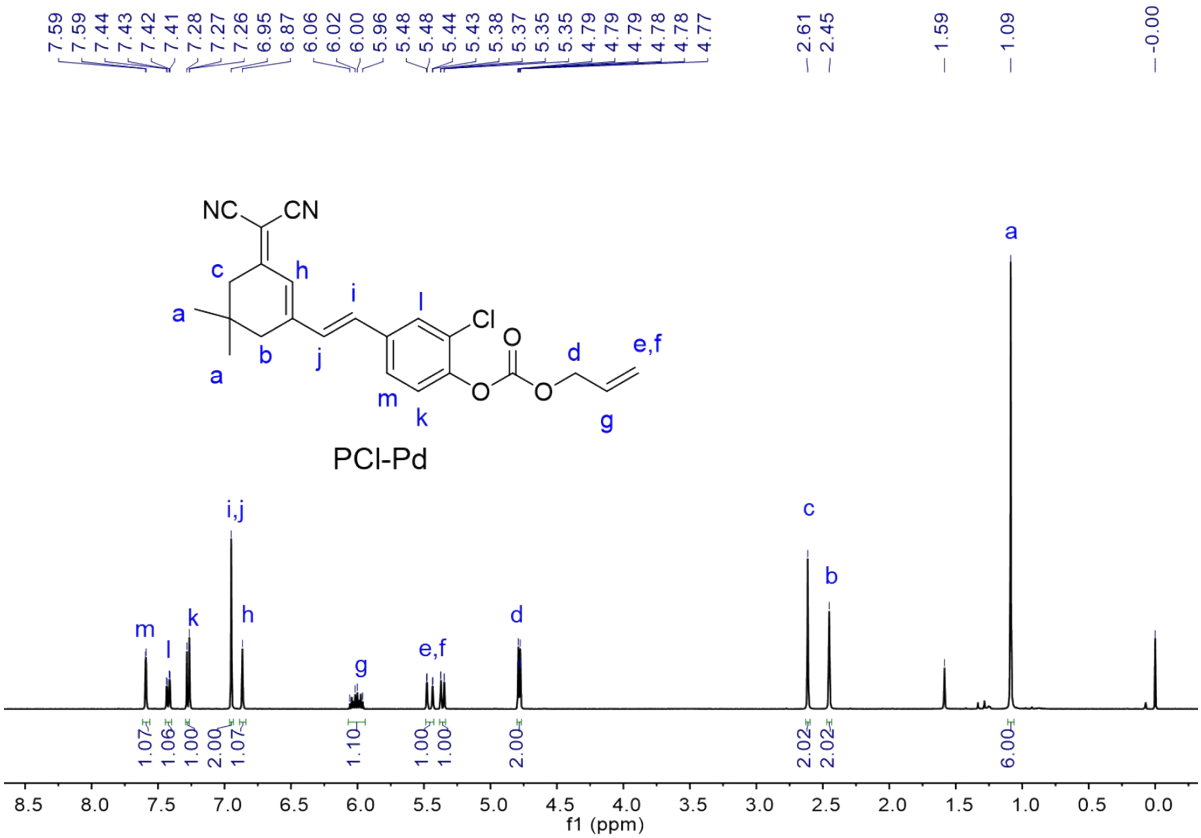

Fig. S23. ^{1}H NMR spectrum of PCl-Pd in $CDCl_3$ (400 MHz, 298 K).

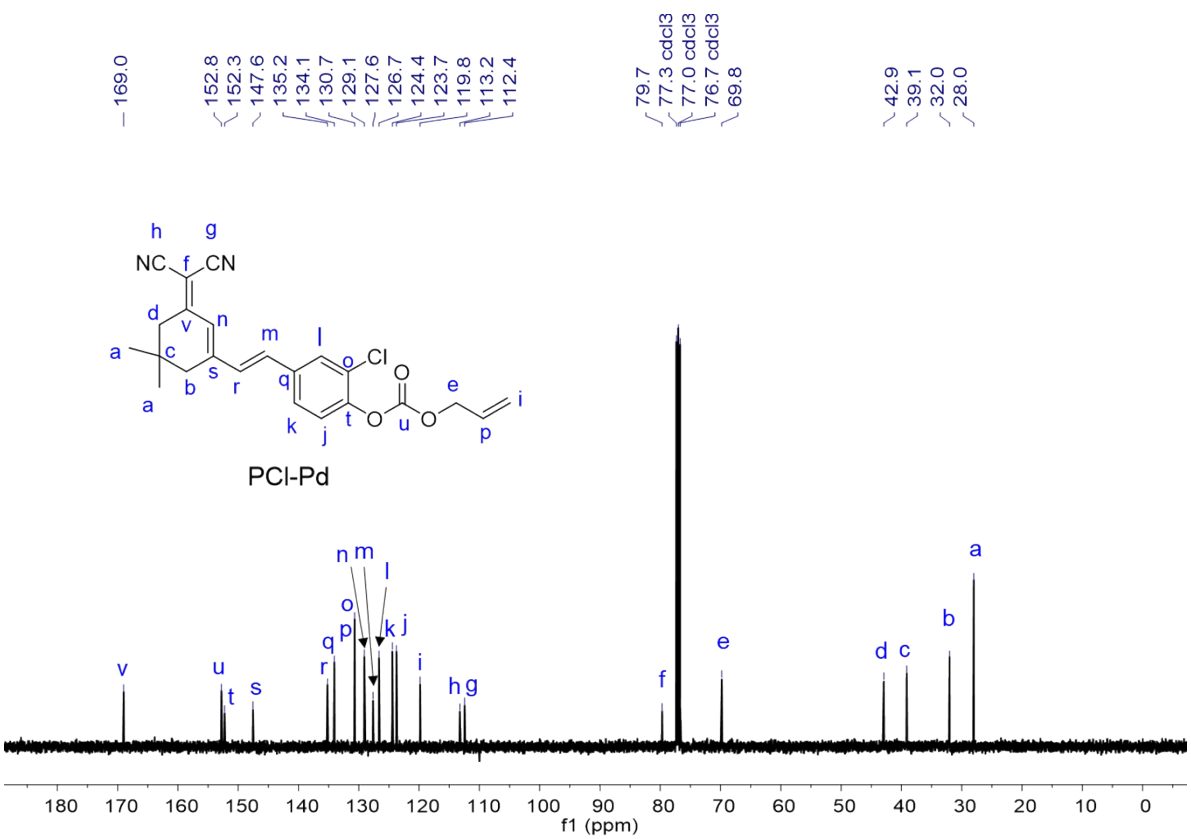

Fig. S24. ^{13}C NMR spectrum of PCl-Pd in $CDCl_3$ (100 MHz, 298 K).

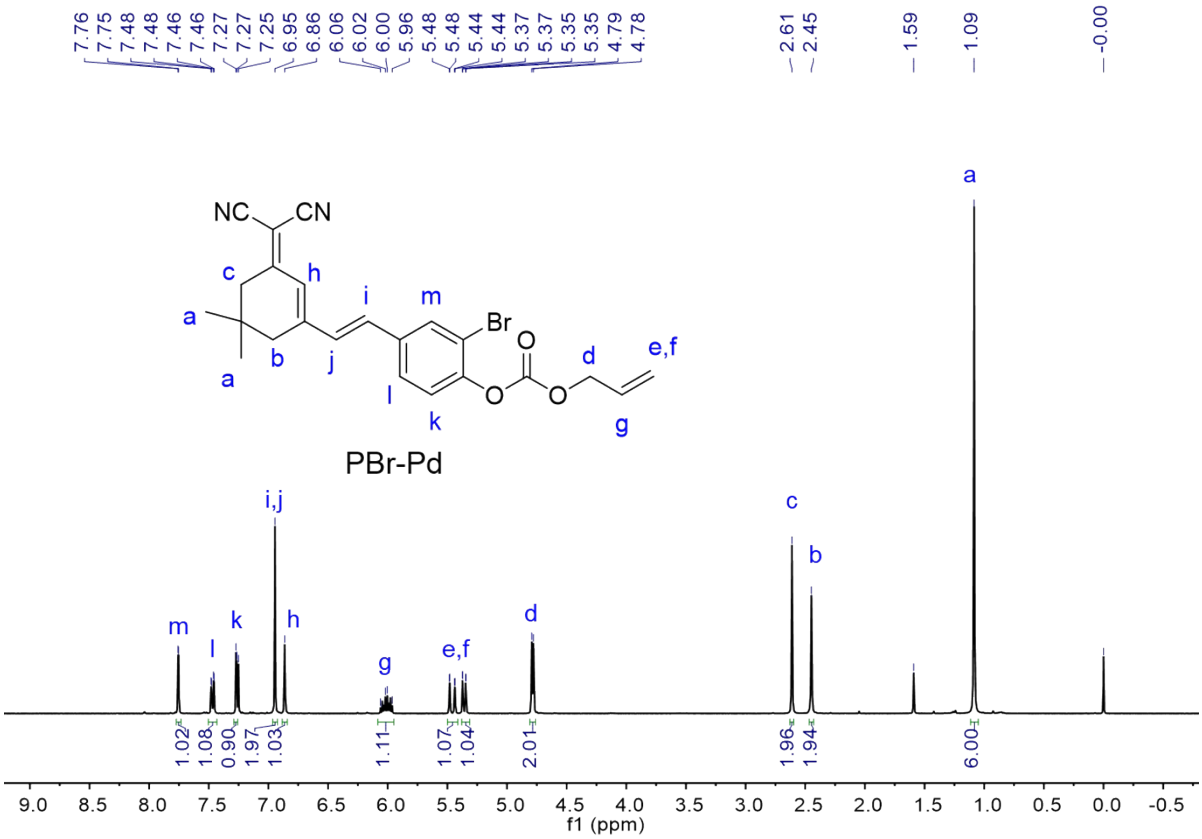

Fig. S25 ^{1}H NMR spectrum of PBr-Pd in $CDCl_3$ (400 MHz, 298 K).

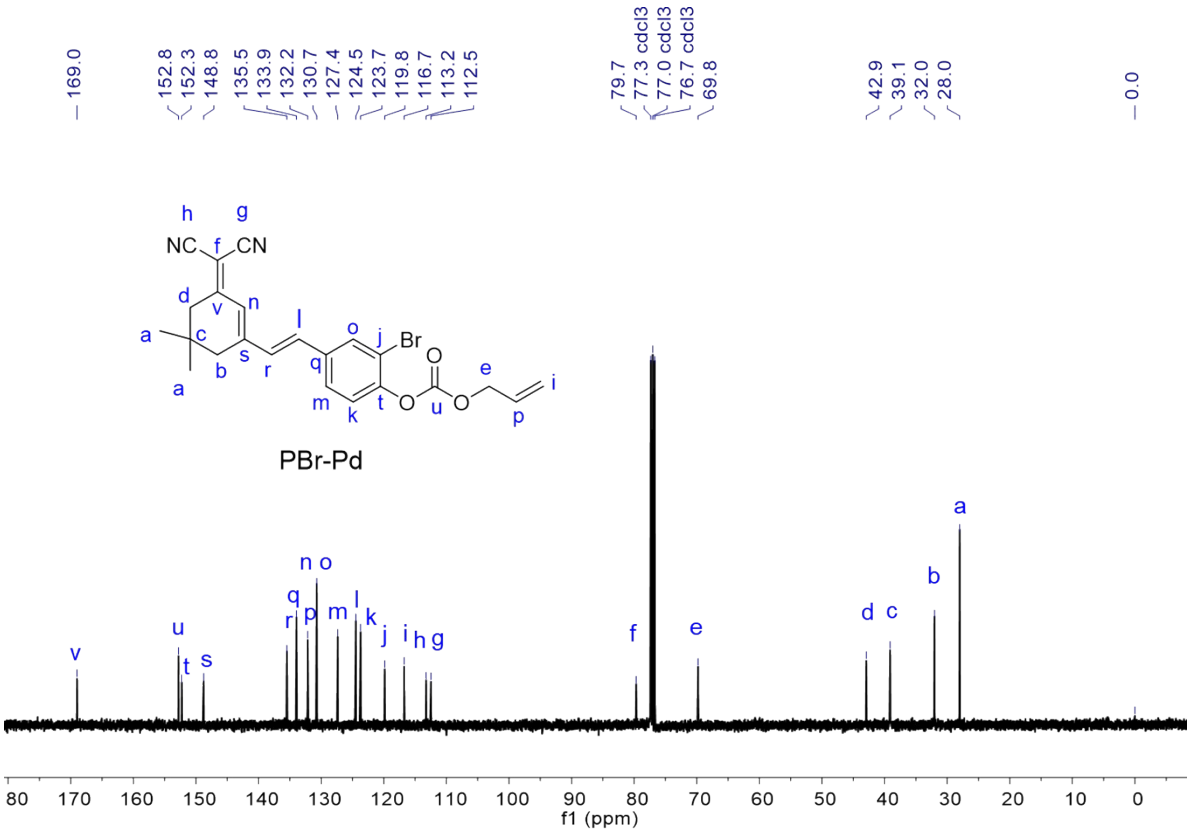

Fig. S26. ^{13}C NMR spectrum of PBr-Pd in $CDCl_3$ (100 MHz, 298 K).

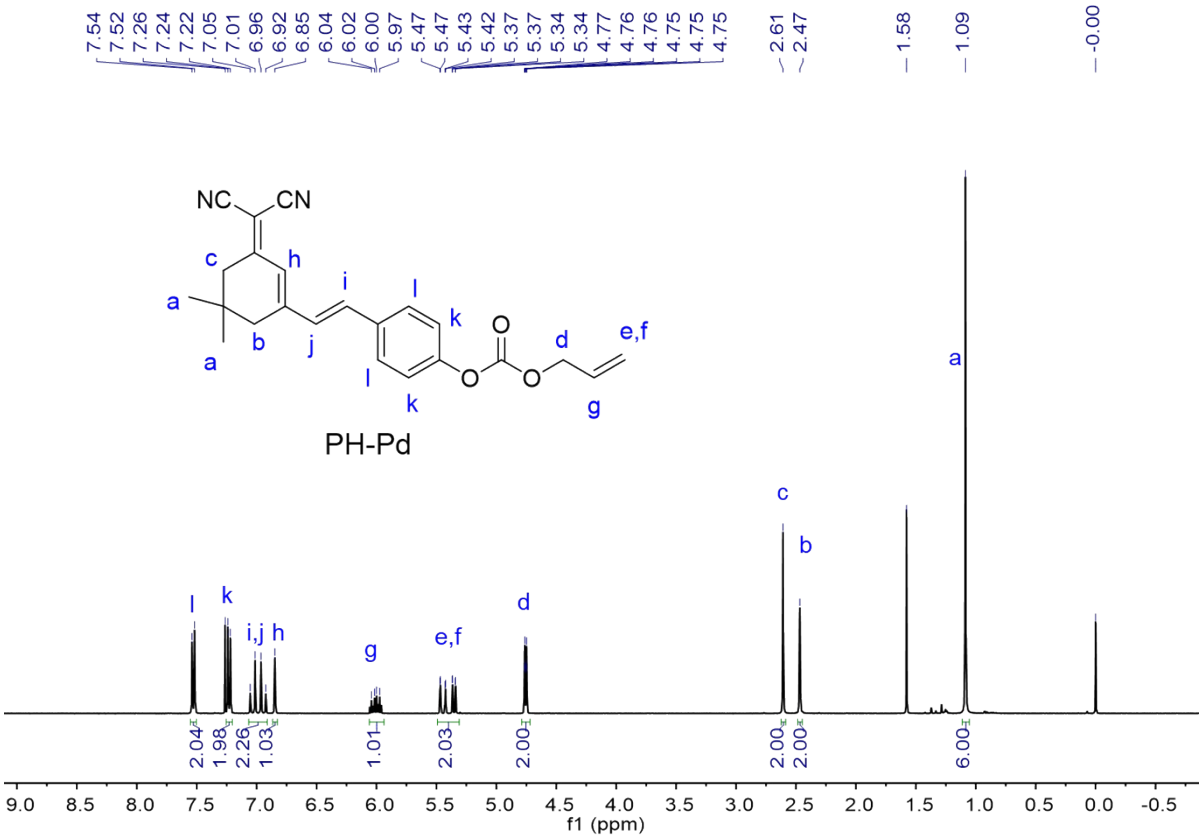

Fig. S27. ^{1}H NMR spectrum of PH-Pd in $CDCl_3$ (400 MHz, 298 K).

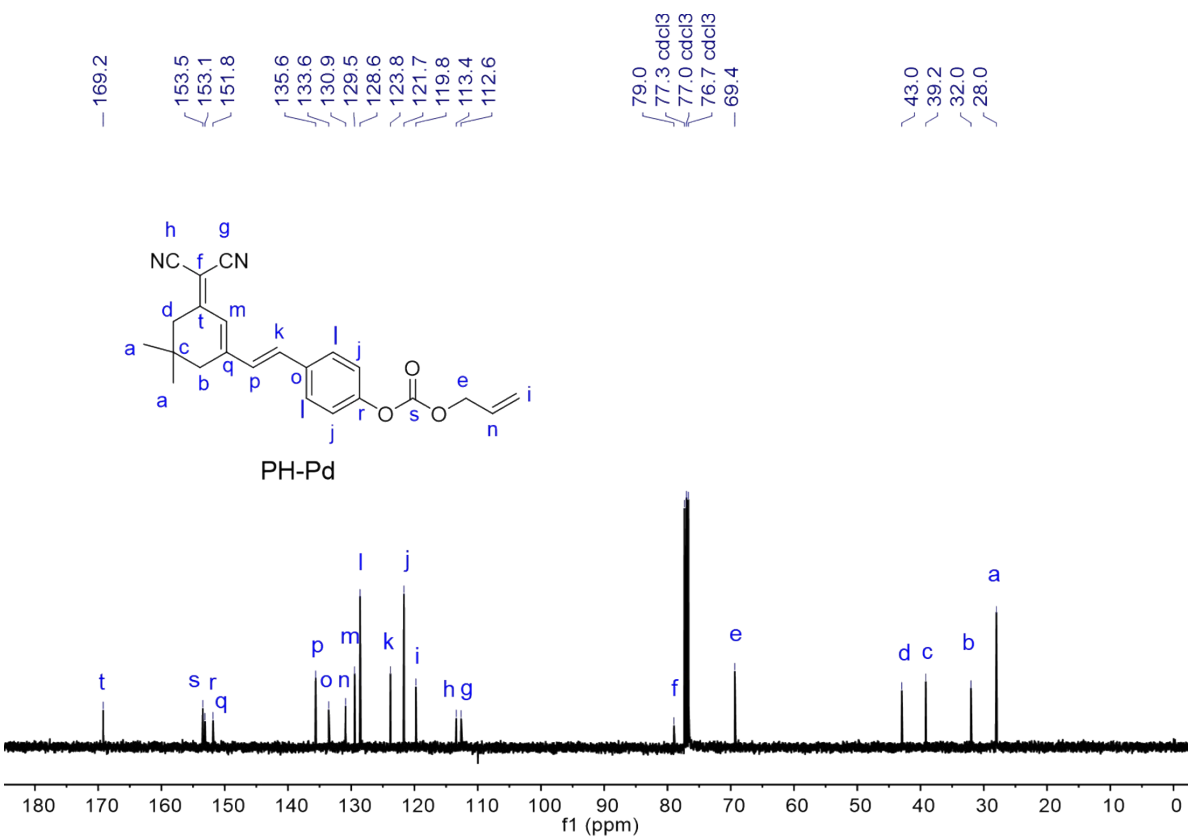

Fig. S28. ^{13}C NMR spectrum of PH-Pd in $CDCl_3$ (100 MHz, 298 K).

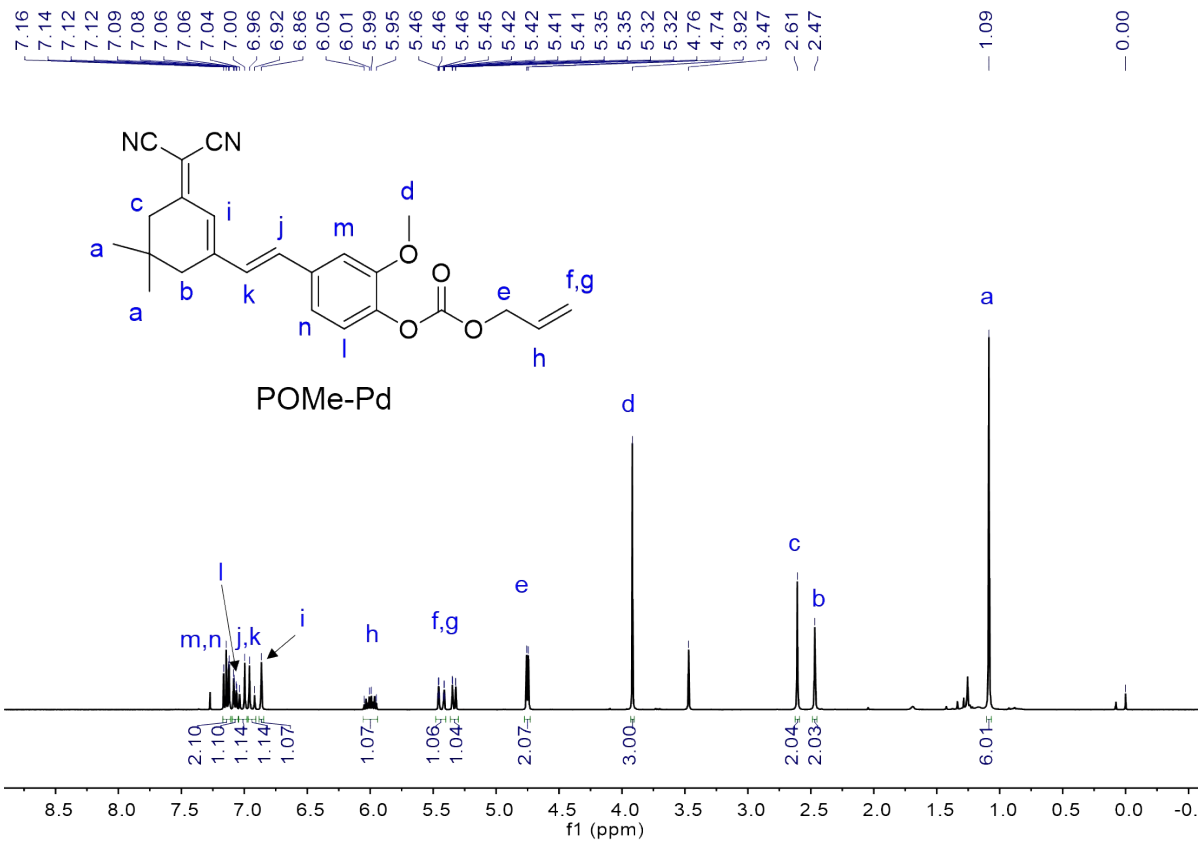

Fig. S29. ^{1}H NMR spectrum of POMe-Pd in $CDCl_3$ (400 MHz, 298 K).

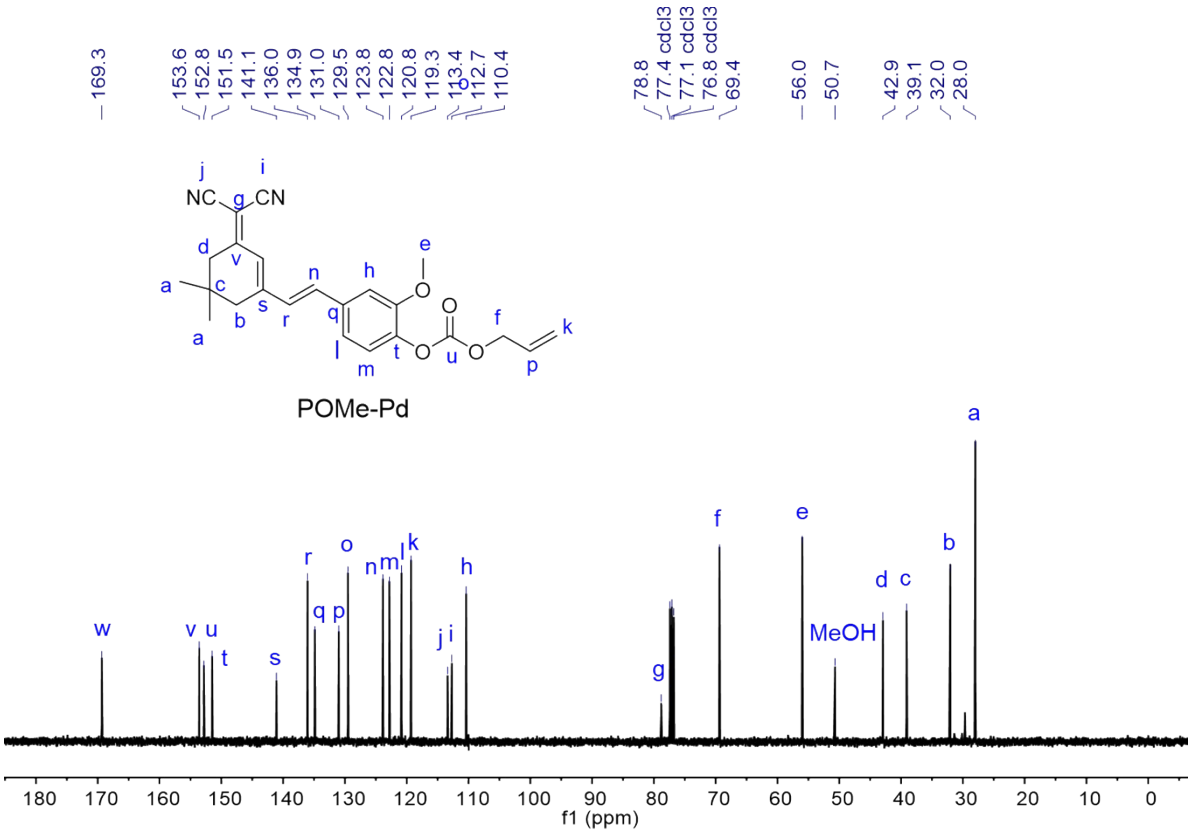

Fig. S30. ^{13}C NMR spectrum of POMe-Pd in $CDCl_3$ (100 MHz, 298 K).

References

1. T. Gao, P. Xu, M. Liu, A. Bi, P. Hu, B. Ye, W. Wang and W. Zeng, *Chem. Asian J.*, 2015, **10**, 1142-1145.
2. L. Zhou, Q. Wang, X.-B. Zhang and W. Tan, *Anal. Chem.*, 2015, **87**, 4503-4507.
3. L. Zhou, S. Hu, H. Wang, H. Sun and X. Zhang, *Spectrochim. Acta A Mol. Biomol. Spectrosc.*, 2016, **166**, 25-30.
4. W. Luo, J. Li and W. Liu, *Org. Biomol. Chem.*, 2017, **15**, 5846-5850.
5. L. Li, R. Guan, M. Guo, P. Ning, R. Shao and X. Meng, *Sens. Actuators, B Chem.*, 2018, **254**, 949-955.
6. W. Feng, L. Bai, S. Jia and G. Feng, *Sens. Actuators, B Chem.*, 2018, **260**, 554-562.
7. J. Zhou, S. Xu, Z. Yu, X. Ye, X. Dong and W. Zhao, *Dyes Pigm.*, 2019, **170**, 107656.
8. L. Wang, M. Ren, Z. Li, L. Dai and W. Lin, *New J. Chem.*, 2019, **43**, 552-555.
9. W. Luo, M. Lei, Y. Wang, H. Gao, Y. Wang, Q. Zhou, Z. Xu and F. Yang, *Anal. Methods*, 2019, **11**, 1080-1086.
10. Z. Ou, L. He, Y. Gao, P. Li, T. Li, J. Zhang, Y. Dong, W. Zhou and Y. Zhang, *New J. Chem.*, 2021, **45**, 5206-5212.
11. X. Li, Y. Liu, X. Li, W. Shi and H. Ma, *Biosens. Bioelectron.*, 2022, **200**, 113929.